nature COMMUNICATIONS

ARTICLE

Received 16 Jul 2012 | Accepted 18 Dec 2012 | Published 5 Feb 2013

DOI: 10.1038/ncomms2396

EAT1 promotes tapetal cell death by regulating aspartic proteases during male reproductive development in rice

Ningning Niu[1,*], Wanqi Liang[1,*], Xijia Yang[1], Weilin Jin[1], Zoe A. Wilson[2], Jianping Hu[3] & Dabing Zhang[1]

Programmed cell death is essential for the development of multicellular organisms, yet pathways of plant programmed cell death and its regulation remain elusive. Here we report that ETERNAL TAPETUM 1, a basic helix-loop-helix transcription factor conserved in land plants, positively regulates programmed cell death in tapetal cells in rice anthers. *eat1* exhibits delayed tapetal cell death and aborted pollen formation. ETERNAL TAPETUM 1 directly regulates the expression of *OsAP25* and *OsAP37*, which encode aspartic proteases that induce programmed cell death in both yeast and plants. Expression and genetic analyses revealed that ETERNAL TAPETUM 1 acts downstream of TAPETUM DEGENERATION RETARDATION, another positive regulator of tapetal programmed cell death, and that ETERNAL TAPETUM 1 can also interact with the TAPETUM DEGENERATION RETARDATION protein. This study demonstrates that ETERNAL TAPETUM 1 promotes aspartic proteases triggering plant programmed cell death, and reveals a dynamic regulatory cascade in male reproductive development in rice.

[1] State Key Laboratory of Hybrid Rice, School of Life Sciences and Biotechnology, Shanghai Jiao Tong University, Shanghai, China. [2] Division of Plant Sciences, School of Biosciences, University of Nottingham, Loughborough, Leics, UK. [3] Department of Energy Plant Research Laboratory, Michigan State University, East Lansing, Michigan, USA. *These authors contributed equally to this work. Correspondence and requests for materials should be addressed to D.Z. (email: zhangdb@sjtu.edu.cn).

In flowering plants, normal development of the anther, the specialized male reproductive organ, is essential to the alternation of life cycle between diploid sporophyte and haploid gametophyte generations.[1,2] Tapetal cells comprise the innermost anther wall layer, which encloses male reproductive cells, and undergo programmed cell death (PCD)-triggered degradation after the meiosis of microspore mother cells. This degradation process is essential for microspore development and pollen wall maturation; as a result, premature or delayed tapetal degradation causes male sterility.

The tapetum is an excellent model system for investigating plant PCD[3]. Several transcriptional regulators have been reported to be associated with tapetal degeneration, including *Arabidopsis* MYB33/MYB65[4], DYSFUNCTIONAL TAPETUM1 (DYT1)[5], DEFECTIVE IN TAPETAL DEVELOPMENT AND FUNCTION1 (TDF1)[6], ABORTED MICROSPORE (AMS)[7], MALE STERILITY1[8], rice GAMYB[9], UNDEVELOPED TAPETUM1[10], TAPETUM DEGENERATION RETARDATION (TDR)[11], PERSISTENT TAPETAL CELL 1 (PTC1)[12], and APOPTOSIS INHIBITOR5 (API5)[13]. However, mechanisms by which these regulators regulate tapetal PCD remain unclear.

PCD is crucial to the development and maintenance of multicellular organisms[14]. Some forms of plant PCD and animal apoptosis (one type of PCD) share several morphological and biochemical similarities, such as fragmentation of genomic DNA, presence of caspase-like proteolytic activities and cytochrome c release from the mitochondria[15–21]. In animals, cysteine aspartyl proteases (caspases) act as a core proteolytic component downstream of many PCD signal pathways[22,23]. Although caspase activities were detected in both animal and plant cells, plant genomes do not have apparent orthologous sequences of caspase genes[15].

Emerging evidence suggests that, in plants and yeast, a novel family of cysteine proteases called metacaspases appears to have endopeptidase activities and shares secondary structural homologies with mammalian caspases[24–29]. The single metacaspase Yeast Caspase-1 (YCA1) in yeast acts as a trigger in ageing and oxidative stress-activated PCD[24]. An *Arabidopsis* metacaspase, mcII-Pa, can cleave a phylogenetically conserved protein, Tudor staphylococcal nuclease, which is also the substrate of mammalian caspase-3, suggesting that some substrates in PCD are conserved between animals and plants[27]. *Arabidopsis* PBA1, one type of the β-subunit of the 20S proteasome, contributes to the caspase-3-like activity during defence response to bacteria in *Arabidopsis*[30]. In addition, aspartic protease is implicated in plant development and cell death. *Arabidopsis UNDEAD*, which encodes an A1 aspartic protease, suppresses tapetal PCD; knockdown of *UNDEAD* causes premature tapetal PCD[31]. Another *Arabidopsis* aspartic protease, PROMOTION OF CELL SURVIVAL1 (PCS1), has an anti-cell death role in embryonic and reproductive development[32]. A third *Arabidopsis* aspartic protease, CONSTITUTIVE DISEASE RESISTANCE 1 (CDR1) is associated with signalling in disease resistance[33]. S5 is the only characterized aspartic protease from rice; its gene is a major locus for *indica–japonica* hybrid sterility[34]. Despite these findings, how aspartic proteases function in plant PCD remains unknown at the mechanistic level.

We previously reported that TDR, the rice ortholog of the *Arabidopsis* AMS protein, is a basic bHLH protein regulating tapetal PCD; *tdr* has expanded tapetal cells and delayed tapetal degeneration. Moreover, TDR is able to directly regulate the expression of a cysteine protease gene *OsCP1*, yet the biochemical role of OsCP1 has not been characterized[11].

To address the mechanism underlying plant PCD and reveal additional regulators of the process, here we report the identification of ETERNAL TAPETUM 1 (EAT1), a key regulator of programmed tapetal development and degradation. Loss of function of *EAT1* results in delayed tapetal PCD and aborted pollen development, causing complete male sterility. *EAT1* encodes a putative bHLH transcription factor that directly regulates the expression of *OsAP25* and *OsAP37*, which encode aspartic proteases that promote cell death. Furthermore, EAT1 has the ability to interact with TDR. This work uncovers novel molecular pathways that determine programmed male reproductive development in plants.

Results

Identification and phenotypic analysis of the *eat1* mutant. To understand the mechanism underlying programmed male reproductive development in the model crop rice, we isolated a new male sterile mutant, *eternal tapetum 1* (*eat1*), from our rice mutant library made from an *O. sativa ssp japonica* cultivar, 9522 (ref. 35). The mutant exhibits normal vegetative development and female organ formation, but is completely male sterile and has shrunken anthers and aborted pollen grains (Fig. 1a–h and Supplementary Fig. S1). All F1 plants of reciprocal crosses between the wild type and the mutant were fertile, and the F2 plants had an approximate 3:1 ratio for phenotypic segregation (fertility: sterility = 160: 47, $\chi^2 = 0.58$, $P > 0.05$, χ^2 test used), suggesting that this male sterile phenotype is caused by a single recessive mutation.

To characterize the cellular abnormality of *eat1-1* during male reproductive development, anther transverse sections were examined. Similar to the wild type, the *eat1-1* mutant anthers appeared to undergo normal meiosis, forming tetrads of haploid microspores at late stage 8 (stage 8b) (Supplementary Fig. S2). Consistent with this observation, normal chromosome separation during meiosis and regular tetrads could be seen in *eat1-1* microspore mother cells, as revealed by 4′,6-diamidino-2-phenylindole staining (Supplementary Fig. S3a). After stage 10, the wild-type tapetal cells had condensed cytoplasm, then became thinner and were eventually degenerated before mature pollen grains were formed (Fig. 1b and c and Supplementary Fig. S2a). In contrast, the *eat1-1* mutant had thicker and darkly stained tapetal cells (Fig. 1f), and abnormal abortion of the anther locule and microspores (Fig. 1g and Supplementary Fig. S2b). These results together show that in the *eat1* mutant, anther development and microspore formation are aborted.

***eat1* exhibits delayed tapetal PCD**. The cellular analysis described above suggests that *EAT1* may affect the degradation of tapetal cells. In plants, tapetal cell degeneration is triggered by PCD, which is characterized by cell condensation, nuclear degeneration and membrane breakdown, and the cleavage of nuclear DNA[11]. To test whether the *eat1* mutant anthers are defective in tapetal PCD, we performed the terminal deoxynucleotidyl transferase-mediated dUTP nick-end labeling (TUNEL) assay and transmission electron microscopy (TEM). Consistent with our previous observations[11], the TUNEL-positive signal in wild-type tapetal cells commenced at stage 8 during late meiosis, became intense at stage 9 when the microspore is released from the tetrad, and weakened at stage 12 when mature pollen grains are formed (Fig. 1d and Supplementary Fig. S3b). However, no obvious DNA fragmentation signal was observed in *eat1* tapetal cells till stage 10, when the vacuolated microspore forms (Fig. 1h and Supplementary Fig. S3b). At stage 11 during mitosis I, weak DNA fragmentation signal was seen in all four layers of the *eat1* anthers (Supplementary Fig. S3b), suggesting delayed and abnormal PCD.

In agreement with results of the TUNEL assays, TEM analysis also revealed a delay in PCD in the mutant (Fig. 2a–h). At stage

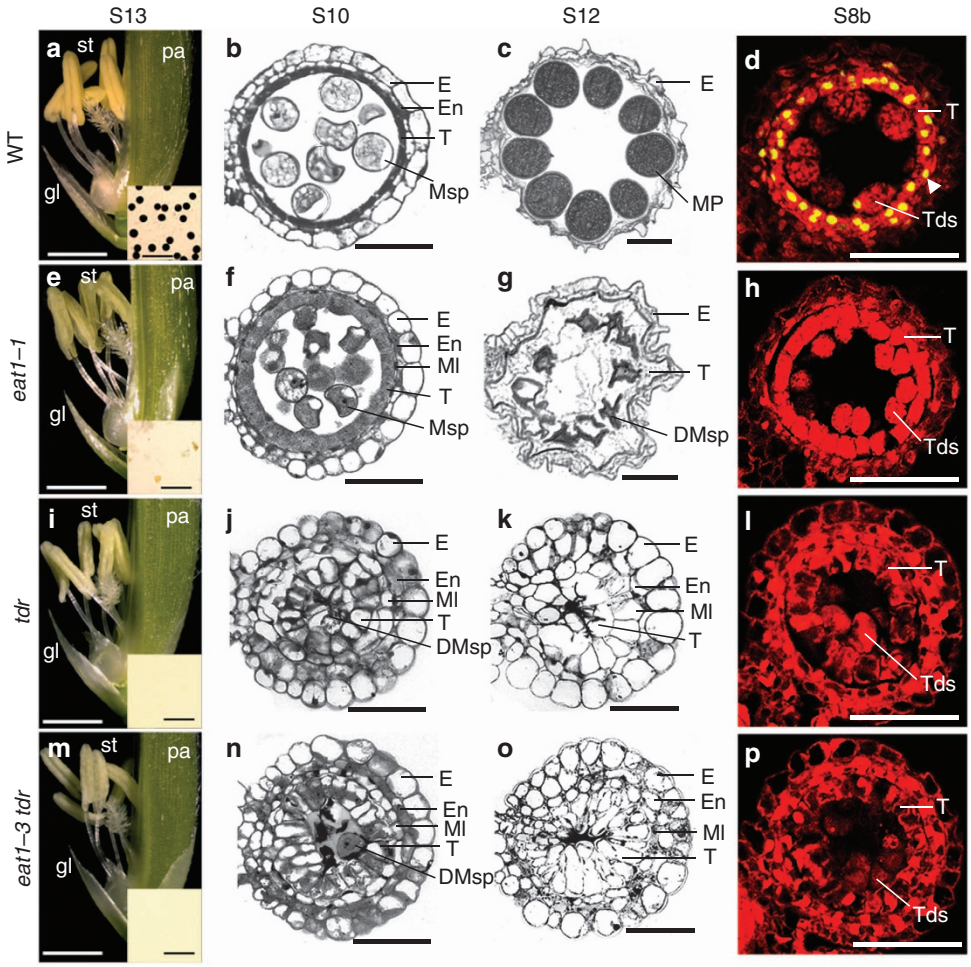

Figure 1 | Phenotypic analysis of anthers of the wild type and mutants. (**a**,**e**,**i**,**m**) Images of rice flowers and (insets) pollen grains stained by iodine-potassium iodide (I_2-KI). Bars, 2 mm for the flowers and 200 μm for insets. (**b**,**c**,**f**,**g**,**j**,**k**,**n**,**o**) Transverse sections of anther locule (bars = 50 μm); (**d**,**h**,**l**,**p**) TUNEL assays (bars, 50 μm). Red signal is PI staining, and yellow fluorescence is the merged signal from TUNEL (green) and PI. Arrow head points out the positive TUNEL signal. Bars, 50 μm. DMsp, degraded microspore; E, epidermis; En, endothecium; gl, glume; Ml, middle layer; MP, mature pollen; Msp, microspore; pa, palea; st, stamen; S8b, stage 8b; S10, stage 10; S12, stage 12; T, tapetum; Tds, tetrads.

10, the wild-type tapetal cells showed typical signs of PCD, such as condensed cytoplasm and the presence of poorly defined organelles (Fig. 2a, e and i). In contrast, *eat1-1* tapetal cells contained abundant distinctive organelles, including the endoplasmic reticulum (ER), Golgi apparatus, a large number of ribosomes attached to the rough-surfaced ER, and an increased number of enlarged mitochondria (Fig. 2b, f and j), suggesting the retention of highly active metabolism and/or delayed cell death processes in the tapetum. At stage 11, the wild-type tapetal cells became more degenerated with the breakage of the nuclear membrane (Fig. 2c, g and k). By contrast, at this stage, the *eat1-1* tapetal cells appeared less disintegrated, with intact nuclear membranes and increased number of mitochondria and vacuoles (Fig. 2d, h and l).

Ubisch bodies are unique structures observed in cereals and other plants, which are proposed to function in exporting tapetum-produced lipidic sporopollenin precursors across the hydrophilic cell wall to the locule for the formation of the lipidic microspore exine[36–38]. At stage 10, the internal surface of the wild-type tapetum contained abundant Ubisch bodies (Fig. 2e and m). In *eat1-1*, however, the Ubisch bodies were abnormally round-shaped and covered by a layer of tubular structures (Fig. 2f and n). As a result, *eat1-1* displayed irregular pollen exine patterning, such as no obvious inter-layer space between the nexine (foot layer) and tectum (Fig. 2o–r). These observations collectively suggest that EAT1 has a key role in tapetal PCD, a process required for microspore development.

***EAT1* encodes a tapetum-expressed bHLH transcription factor.** Map-based cloning was used to identify the *EAT1* gene. Using 120 mutant individuals from the F2 population of a cross between *eat1*-1 and Guang Lu Ai (an *indica* variety), the *EAT1* gene was mapped to chromosome 4 between XY409-4 and XY409-5, two Insertion-Deletion markers that define a 3-cM (centimorgan) DNA region (Fig. 3a). While sequencing anther-expressed candidate genes within this region, we found deletions of the 543rd and 544th nucleotides (T and G) in the coding region of a gene that corresponded to LOC_Os04g51070 (http://www.gramene.org/, also annotated as Os04g0599300 by http://rapdb.dna.affrc.go.jp/) (Fig. 3b). From the Tos17-insertion mutant library (Rice Genome Resource Center, RGRC), we later identified two additional alleles, *eat1-2* and *eat1-3* (Fig. 3b and Supplementary Fig. S1e), both of which also showed male sterility (Supplementary Fig. S1a–d) and delayed cell death in the tapetum (Supplementary Fig. S3b).

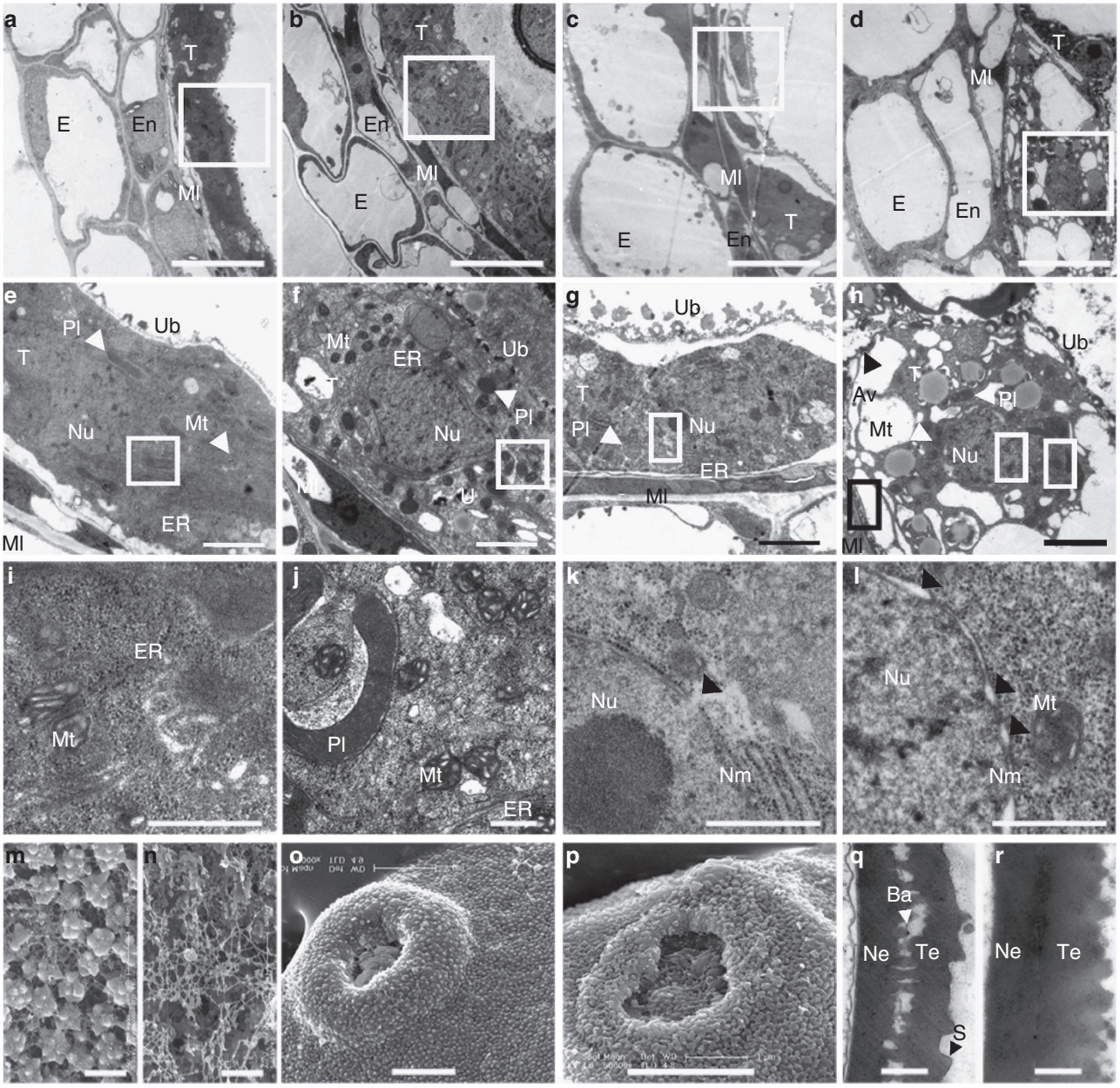

Figure 2 | Electron micrographs of anthers and pollen grains. The transverse section of anthers at early stage 10 (10a) (**a**,**b**) and stage 11 (**c**,**d**). The tapetal cells of stage 10a (**e**,**f**) and stage 11 (**g**,**h**) are high magnifications of the insets of (**a**–**d**). (**i**,**j**) Higher magnification of the insets of (**e**,**f**) showing mitochondria (Mt) and endoplasmic reticulum (ER). (**k**,**l**) Higher magnification of the insets of (**g**,**h**) showing the nuclear membranes. (**k**) Disintegration of the wide-type nuclear membrane, where the breakage is marked by the black arrowhead. (**l**) The *eat1-1* nuclear membrane was intact and partially widened, marked by the black arrowhead. (**m**–**p**) Scanning electron microscopic analysis of the inner surface of the tapetal layer (**m**,**n**) and pollen grains (**o**,**p**) at stage 10. (**q**–**r**) Transverse section of the exine of microspore wall at stage 11, showing tectum, nexine, bacula (white arrow head) and spine distribution on the exine. (**a**,**c**,**e**,**g**,**i**,**k**,**m**,**o**,**q**) Wild type. (**b**,**d**,**f**,**h**,**j**,**l**,**n**,**p**,**r**) *eat1-1*. Bars, 5 μm in (**a**–**d**), 2 μm in (**e**–**h**,**o**,**p**) and 500 nm in (**i**–**n**,**q**,**r**). (**e**,**f**,**g**,**h**,**j**,**k**,**l**) Were high. As, abnormal secretion; Av, abnormal vacuole; Ba, bacula; E, epidermis; En, endothecium; Ml, middle layer; Mt, mitochondria; Ne, nexin; Nm, Nuclear membranee; Nu, nucleus; Pl, plastid; S, spine; T, tapetum; Te, tectum; Ub, ubisch body.

We further investigated the spatio-temporal expression pattern of the *EAT1* gene by qualitative and quantitative RT–PCR (qRT–PCR) analyses. In the wild type, *EAT1* is weakly expressed in roots, shoots and leaves, and highly expressed in the anther from stage 7 to 12, while a dramatic reduction in expression was detected in the anthers in all three *eat1* alleles (Fig. 3c). In GUS-stained $EAT1_{pro}$:*GUS* transgenic flowers, GUS signals started to appear in anthers at stage 7, became stronger from stage 8 to 9, and were nearly undetectable at stage 12 (Fig. 3d). Further transverse section analysis of GUS-stained locules and *in situ* RNA hybridization indicated that *EAT1* is highly expressed in the tapetum (Fig. 3d and e). Previous studies suggested that tapetal PCD is initiated at stage 8 during the meiosis of microspore mother cells[11], thus the spatio-temporal expression pattern of *EAT1* is in good agreement with a potential role of this protein in tapetal PCD.

EAT1 acts downstream from and interacts with TDR. To understand the role of EAT1 in the regulatory network of tapetal

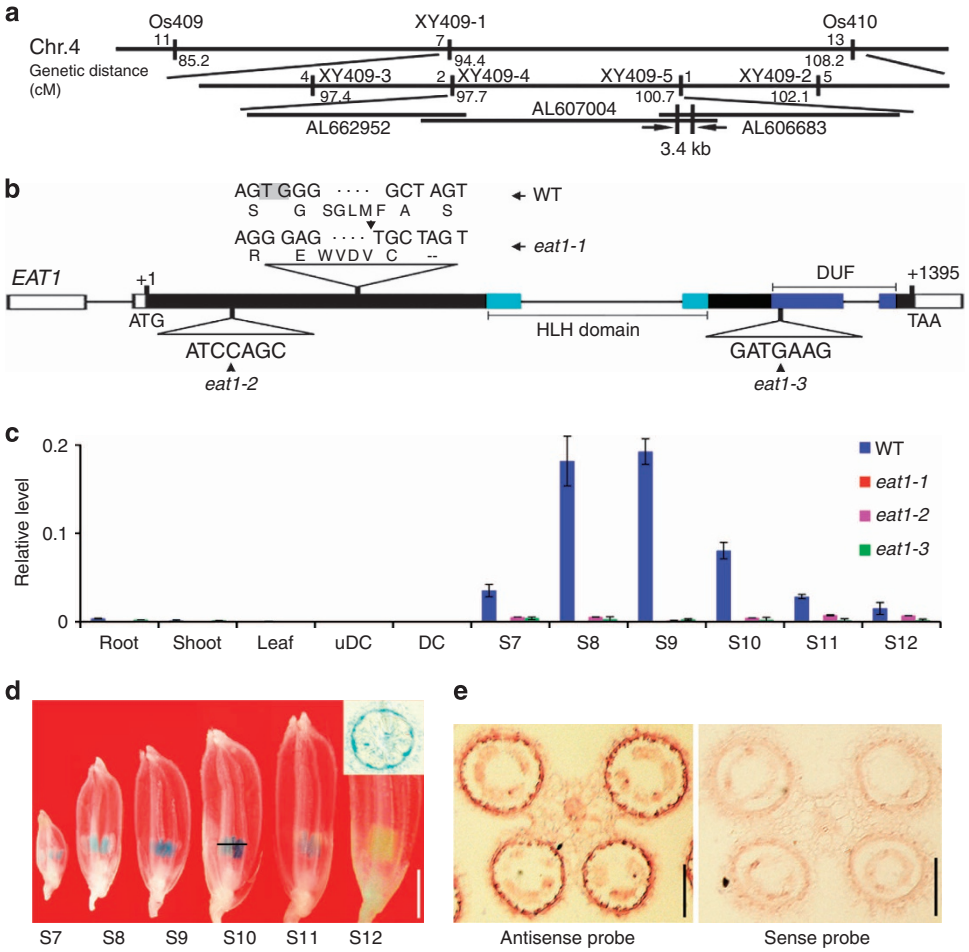

Figure 3 | Identification and expression analyses of *EAT1*. (**a**) Fine mapping of *eat1-1* to chromosome 4. Names and positions of the molecular markers are indicated. AL662952, AL607004 and AL606683 are rice genomic DNA accession numbers of bacterial artificial chromosome clones. (**b**) A schematic representation of *EAT1*. (**c**) *EAT1* expression analysis by qRT-PCR. One-way analysis of variance test was used. Results are presented as mean ± s.e. (**d**) GUS staining of transgenic anthers containing $EAT1_{pro}$:*GUS*; bar, 2 mm. Inset, GUS staining in a transverse section of a stage 10 anther locule (as indicated by the black horizontal bar); bar, 50 μm. (**e**) *In situ* analysis of *EAT1* in wide-type anthers at stage 8. Bars, 50 μm. uDC, undifferentiated callus; DC, differentiating callus; S7 to 12, Stage 7 to 12.

development, the expression level of several genes encoding transcriptional regulators or Leu-rich repeat receptor-like protein kinase in this process was examined by qRT–PCR. Genes such as *MULTIPLE SPOROCYTE* (*MSP1*)[39], *GAMYB*[9], *UDT1*[10], *TDR*[11], *PTC1*[12], and *API5*[13] showed no obvious changes in *eat1-1* anthers (Supplementary Fig. S4a–f). *OsCP1*, a cysteine protease-encoding gene[40] that is directly regulated by TDR and API5[11,13], exhibited a slight reduction in expression until stage 10, and an increase in expression after stage 11 (Supplementary Fig. S4g). Conversely, the expression of *EAT1* was slightly decreased in *gamyb1–4* and *udt1*, and greatly reduced in *tdr* and *ptc1* (Supplementary Fig. S4h), suggesting that TDR and PTC1 may positively regulate the expression of *EAT1*.

Previously we showed that TDR is a positive transcriptional regulator in tapetal PCD[11]. To determine the relationship between *EAT1* and *TDR*, we constructed the *eat1-3 tdr* double mutant. Histological analyses showed that *eat1-3 tdr* displayed defective anther development, including delayed tapetal degeneration, enormously expanded tapetal cells and negative TUNEL signal (Fig. 1m–p and Supplementary Fig. S3b), similar to the phenotype of *tdr* (Fig. 1i–l and Supplementary Fig. S3b). We thus propose that EAT1 functions in one of the pathways controlled by TDR and that TDR may regulate the expression of *EAT1*.

Our previous studies showed that two *Arabidopsis* bHLH proteins, AtbHLH089 and AtbHLH091, interact with AMS, the ortholog of TDR in *Arabidopsis*[7]. EAT1 shares sequence similarity with AtbHLH089 and AtbHLH091[41]. To gain further insight into the function of EAT1, we performed a yeast two-hybrid analysis to determine whether EAT1 interacts with TDR. Yeast strains coexpressing EAT1 and TDR grew normally under stringent selection conditions (30 mM 3-amino-1, 2, 4-triazole) and displayed activation of the expression of *HIS3*, *ADE2* and the *LacZ* reporter genes, confirming the interaction between EAT1 and TDR (Fig. 4a). *In vitro* interaction between these two proteins was further confirmed using co-immunoprecipitation (Co-IP) assays (Fig. 4b). Furthermore, we validated this interaction using bimolecular fluorescent complementation (BiFC) in rice protoplasts. In contrast to the negative control, yellow fluorescent protein (YFP) signals were observed in the nucleus of the cells expressing EAT-nYFP and TDR-cYFP (Fig. 4c), confirming the interaction of the two proteins *in vivo*. In support of these data, *TDR* is also highly expressed in the tapetum[11].

***EAT1* is conserved in terrestrial plants**. To understand the evolution of *EAT1*, we used the full-length EAT1 protein

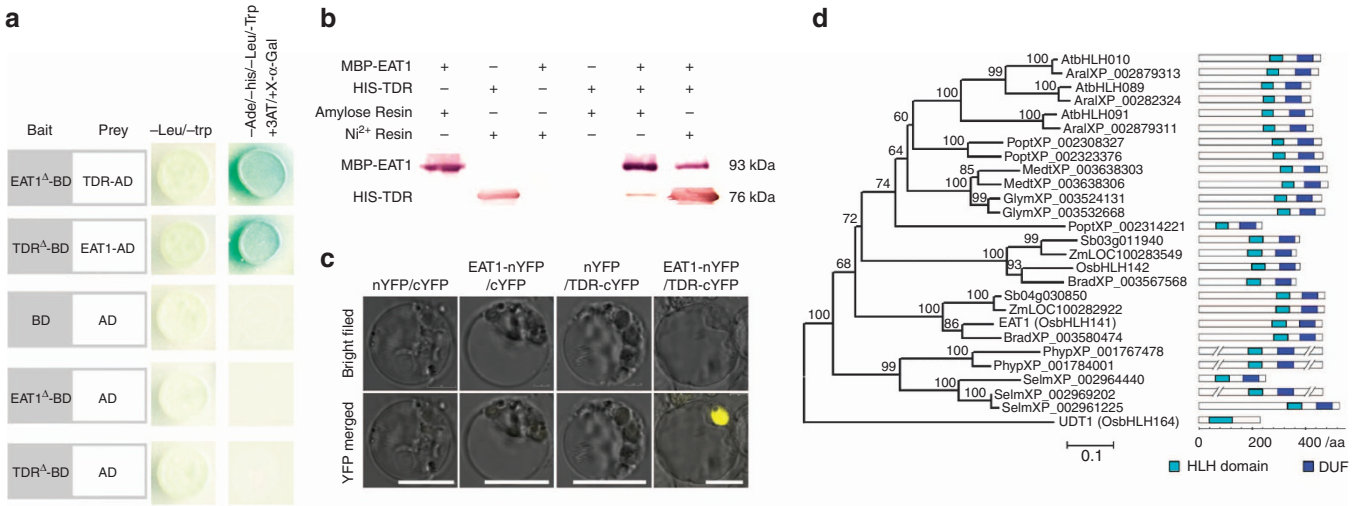

Figure 4 | EAT1 interacts with TDR and phylogenic analysis of *EAT1*. (**a**) EAT1 and TDR interact in yeast cells. Co-expression of EAT1 and TDR was able to activate the expression of the *HIS3, ADE2* and *LacZ* reporter genes. (**b**) Co-IP of MBP-EAT1 and HIS-TDR recombinant proteins expressed in *E. coli*. Maltose-binding protein (MBP) alone and HIS alone were used as negative controls. (**c**) BiFC in rice protoplasts expressing the indicated constructs. Bars, 10 μm. (**d**) A neighbour-joining tree of EAT1 and its homologues. Aral, *Arabidopsis lyrata;* At, *Arabidopsis thaliana*; Brad, *Brachypodium distachyon;* Glym, *Glycine max*; Medt, *Medicago truncatula*; Os, *Oryza Sativa*; Phyp, *Physcomitrella patens*; Popt, *Populus trichocarpa;* Sb, *Sorghum bicolours*; Selm, *Selaginella moellendorffii;* Zm, *Zea may.*

sequence to search available public databases and retrieved a total of 26 homologues from 10 diverse plant species from moss, pteridophytes, to angiosperms (Fig. 4d and Supplementary Tables S1 and S2). The molecular functions of these homologues have not been reported.

Phylogenetic analysis showed that EAT1 and the 26 homologues each have a single HLH domain and a conserved but previously uncharacterized motif at the C-terminus, designated as DUF for Domain of Unknown Function (Figs 3b and 4d and Supplementary Fig. S5 and Table S2). Moreover, *EAT1* and three homologues from *Sorghum bicolour* (Sb04g030850), *Zea mays* (ZmLOC100282922) and *Brachypodium distachyon* (BradXP_003580474), respectively, were grouped in a subclade (Fig. 4d), suggesting that EAT1 and its homologues underwent diversification during grass evolution. EAT1 has one homologue from rice (OsbHLH142), which shares 40.8% identity with EAT1 in the HLH and DUF domains, and three homologues from *Arabidopsis* (AtbHLH091, AtbHLH089, AtbHLH010), which share an average of ~40% identity with EAT1 in these two conserved domains (Fig. 4d and Supplementary Fig. S5). In addition, seven of the *EAT1* homologues identified from *Medicago truncatula*, *Populus trichocarpa*, *Glycine max*, *Arabidopsis* and rice are also expressed in reproductive organs, such as inflorescences and male organs (Supplementary Table S1). These findings suggest a specific and possibly conserved role for *EAT1* in male reproductive development in plants.

EAT1 directly regulates the expression of aspartic proteases. To understand the mechanism of *EAT1*'s function in gene expression during tapetal PCD and microspore development, we performed microarray analysis of *eat1* at stage 9 of anther development, and observed changes in the expression of many genes (data not shown). Among them, two aspartic protease-encoding genes, *OsAP25* and *OsAP37*, showed a significant reduction in expression, which was further confirmed by qRT–PCR (Fig. 5a and Supplementary Fig. S6a and b). Interestingly, the expression of these two genes is also greatly reduced in *tdr* (Supplementary Fig. S6b), the mutant of another transcription factor involved in rice tapetal PCD[11] (see previous section). Therefore, we chose to focus on *OsAP25* and *OsAP37* to determine whether these genes are directly regulated by EAT1 in PCD.

Given that bHLH transcription factors are predicted to regulate gene expression by binding to the E-box (CANNTG) in the promoter of target genes[7], we used chromatin immunoprecipitation (ChIP)-PCR and electrophoretic mobility shift assay (EMSA) assays to test whether EAT1 could directly regulate *OsAP25* and *OsAP37*. EAT1 polyclonal antibodies were generated using an EAT1-specific peptide fragment (see Methods), and their specificities were confirmed using protein gel blot analysis (Supplementary Fig. S7a) before the antibodies were used in ChIP-PCR. Results from ChIP-PCR and EMSA demonstrated that EAT1 binds to the E-box-containing promoters of *OsAP25* and *OsAP37* (Fig. 5b and c). In contrast, we did not observe an obvious association of EAT1 with the promoter of the control gene *OsAP19*, which only displayed a slight reduction in expression in *eat1-1* (Supplementary Fig. S7b and c). These data suggest that EAT1 directly regulates the expression of these two aspartic protease genes.

Consistent with a role of EAT1 in regulating *OsAP25* and *OsAP37*, all three genes were highly expressed in tapetal cells (Fig. 3c–e and Fig. 5a and Supplementary Fig. S6c). One tissue in which *EAT1* and *OsAP25* were differentially expressed was the callus, where *OsAP25* transcripts were observed yet no *EAT1* expression signals were seen, suggesting a possible separate role for *OsAP25* in rice regeneration (Fig. 3c and Supplementary Fig. S6a). In agreement with this hypothesis, we were unable to use the artificial microRNA technology to obtain transgenic plants via calli to suppress the expression of *OsAP25* (data not shown).

OsAP25 and OsAP37 activate cell death in yeast. To characterize the potential role of OsAP25 and OsAP37 in PCD, *GAL10* promoter-driven *OsAP25* and *OsAP37* were individually transformed into a PCD-deficient yeast strain, *Δyca1*[23]. After 4-h 20 mM H_2O_2 treatment, 82% and 71% of the yeast cells overexpressing *OsAP25* and *OsAP37*, respectively, displayed positive signals when labelled with the mammalian caspase

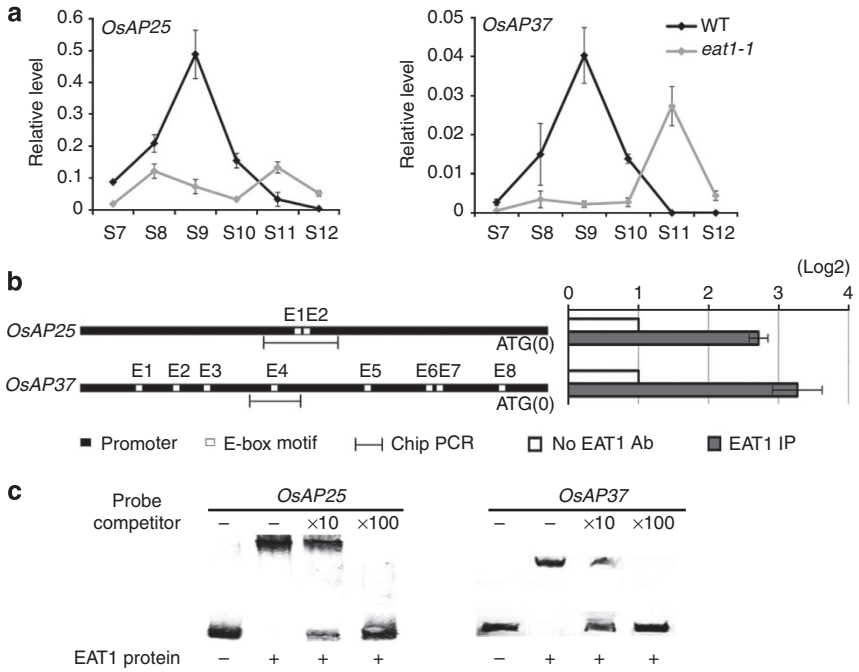

Figure 5 | Analysis of genes regulated by *EAT1*. (**a**) qRT-PCR analysis of *OsAP25* and *OsAP37*. (**b**) Presence of the E-box motifs in the promoters of *OsAP25* and *OsAP37* (left) and qChIP-PCR results (right) showing preferred binding of EAT1 to the promoter fragments containing the E-box motifs, that is, E1E2 on *OsAP25* and E4 on *OsAP37*. (**c**) EMSA assay showing the binding of recombinant EAT1 to the promoter fragments of *OsAP25* and *OsAP37*. The binding complex could be outcompeted by increasing quantities of unlabelled DNA fragments (× 10 and × 100 of unlabelled DNA fragments). One-way analysis of variance test was used. Results are presented as mean ± s.e. E(n), E-box motif; EAT1 IP, immunoprecipitated chromatin by EAT1 antibody; No EAT1 Ab, negative control without EAT1 antibody; S7 to 12, Stage 7 to 12.

substrate FITC-VAD-fmk, suggesting that OsAP25 and OsAP37 share a similar function with YCA1 in promoting PCD process in yeast (Fig. 6a). Eight hours after the H_2O_2 treatment, propidium iodide (PI) staining and flow cytometry analysis were performed to measure the number of live cells. Whereas 93% of the non-transformed *Δyca1* cells were still alive, cells overexpressing *OsAP25* and *OsAP37* had a survival rate of 18% and 29%, respectively (Fig. 6b). These findings suggest that, similar to the yeast metacaspase protein YCA1[24], OsAP25 and OsAP37 have the ability to promote cell death in yeast cells.

Overexpression of OsAP25/37 leads to cell death in plants. To further test the roles of the aspartic proteases in cell death, we expressed the full-length CDS of *OsAP25* or *OsAP37* driven by the *CAMV 35S* promoter in plants. Trypan blue vital staining of tobacco leaves revealed substantially increased death of epidermal and mesophyll cells in leaves transiently expressing OsAP25 or OsAP37 compared with those expressing green fluorescent protein (GFP), or OsAP25 and OsAP37 together with the aspartic protease-specific inhibitor pepstatin A (penetratin, PepA-P) (Fig. 6c). Furthermore, overexpression of *OsAP25-GFP* in *Arabidopsis* caused the death of 53% of the transgenic seedlings 15 days after seed germination and left ~85% of the plants dead by 35 days (Fig. 6d). No stable transgenic lines overexpressing *OsAP37* were obtained, indicating that overexpression of *OsAP37* may block early plant development or cause premature death. Consistent with these results, *Arabidopsis* transgenic lines expressing inducible *OsAP25* or *OsAP37* exhibited extensive cell death (indicated by Trypan blue staining) in leaves and cotyledons 48 h after their gene expression was induced by estradiol (Fig. 6e).

Discussion

In this study, we have revealed an essential role of EAT1 in programmed tapetal cell death and pollen formation in the monocot crop rice. By *in vivo* and *in vitro* analyses, we show that EAT1 directly regulates the expression of two aspartic protease genes that promote cell death in yeasts and plants. Additionally, genetic and molecular analyses suggest that EAT1 acts downstream of TDR in triggering cell death, and that EAT1 can also form a protein complex with TDR. These findings suggest that EAT1 and TDR represent two key factors in the regulatory network of anther development in rice and that one pivotal role for EAT1 is to regulate the expression of aspartic protease genes.

Both plant and yeast cells have morphological and biochemical PCD features similar to that of animal apoptosis. Furthermore, plant cell death can be blocked by human caspase inhibitors, and caspase-like activities were detected in plants[18–21,30,42]. In this study, we showed that two aspartic proteases, OsAP25 or OsAP37, can rescue the yeast metacaspase-deficient strain, *Δyca1*. Ectopic expression of *OsAP25* or *OsAP37* promotes cell death in plants as well, and treatment with aspartic protease-specific inhibitor significantly reduced this effect. These results suggest that a subset of plant aspartic proteases also function as executors in PCD, indicating possible mechanistic similarities between apoptosis in animals and PCD in yeast and plants. However, although yeast metacapase mutant strains expressing *OsAP25* or *OsAP37* could be labelled by the caspase substrate FITC-VAD-fmk (Fig. 6a), we were unable to detect caspase-1-9 activities in mammalian cell extracts expressing *OsAP25* or *OsAP37* (data not shown). This result may reflect the fact that these aspartic proteases have target proteins or cleavage motif distinct from animal caspases.

Although YCA1 was initially reported to have caspase-like activity[24], subsequent studies showed that Arabidopsis

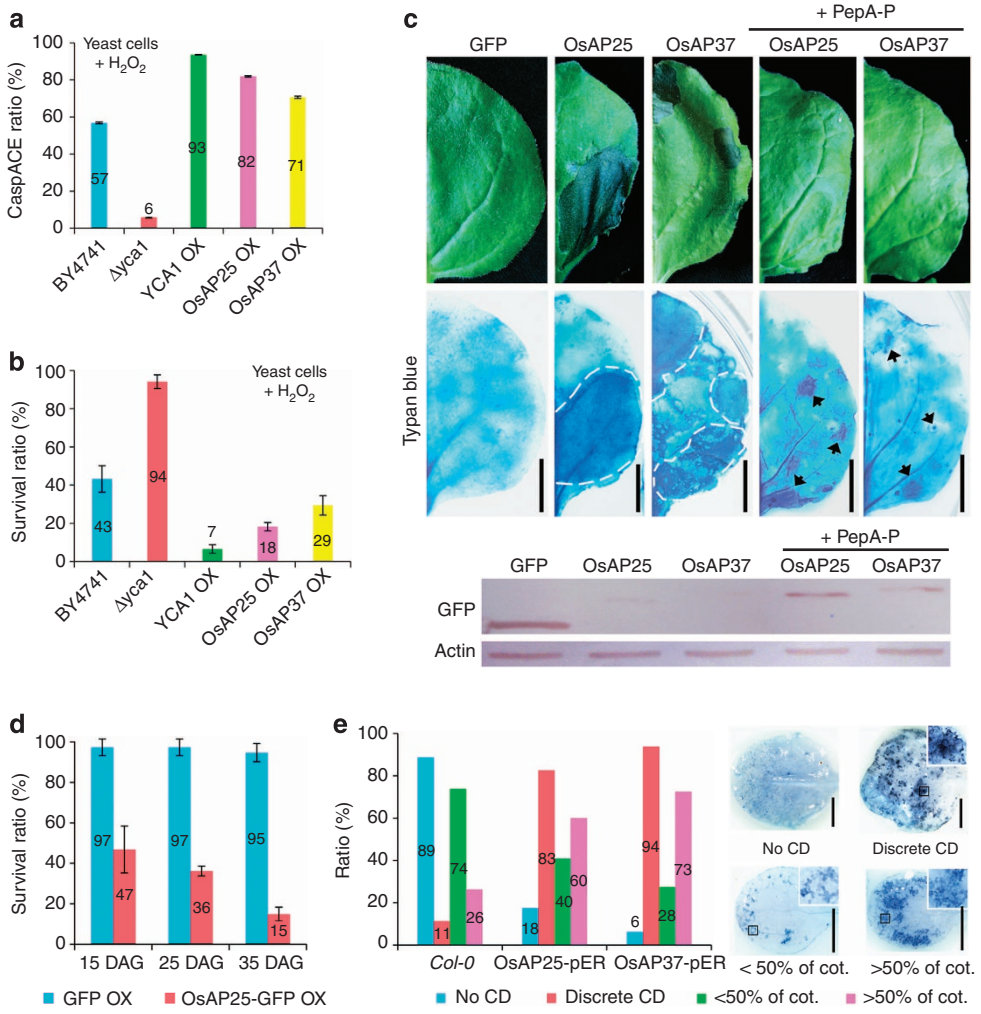

Figure 6 | OsAP25 and OsAP37 promote PCD in yeast and plants. (**a**) FITC-VAD-fmk staining showing caspase activities in yeast strains. (**b**) Survival rates of yeast cells overexpressing *OsAP25* and *OsAP37* as shown by PI staining. (**c**) Tobacco leaves transiently expressing *GFP*, *OsAP25-GFP* or *OsAP37-GFP* and were stained by Trypan blue. The dead epidermal cells are indicated by dashed lines and arrows. Bars, 1 cm. Below the leaf images is the western blot analysis of extracts of tobacco leaves transiently expressing *GFP*, *OsAP25-GFP* or *OsAP37-GFP*, using the GFP antibody. (**d**) Survival rates of *Arabidopsis* seedlings overexpressing *OsAP25-GFP*, 15, 25 and 35 days after germination. (**e**) Quantification of Trypan blue staining in leaves and cotyledons of transgenic seedlings expressing oestrogen-induced *OsAP25* (*OsAP25-pER*) or *OsAP37* (*OsAP37-pER*) 48 h after estradiol treatment. Bars, 1 mm. The insets are higher magnifications of the boxed regions. $n = 78$ for cotyledons and 80 for leaves. One-way analysis of variance test was used. Results are presented as mean ± s.e. CD, cell death of leaf; DAG, days after germination; discrete CD, dotted distribution of cell death on the leaf; NO CD, no cell death detected; PepA-P, Pepstatin A; <50% of cot., extensive cell death covering <50% of the cotyledon; >50% of cot., extensive cell death covering >50% of the cotyledon.

metacaspases AtMCP1b and AtMCP2b, as well as yeast YCA1, exhibit arginine/lysine-specific endopeptidase activities with no direct cleavage activity on caspase-specific substrates[25], suggesting that the metacaspases may activate downstream effective caspase-like protease(s) involved in cell death[25]. Consistent with this, crystal structure analysis revealed that even though the YCA1 metacaspase has a caspase-like fold, the protein exists as a monomer both in solution and in crystals, instead of forming homodimers like canonical caspases[29]. We thus propose that OsAP25 and OsAP37 may activate downstream caspase-like protease(s) involved in PCD rather than directly acting on caspase-specific substrates. Moreover, even though OsAP25, OsAP37, PCS1 and UNDEAD belong to the C-group of aspartic proteases[43,44], OsAP25 and OsAP37 can promote cell death (Fig. 6b–e) whereas UNDEAD and PCS1 have anti-PCD functions[31,32], suggesting diversified roles of aspartic proteases in plant PCD.

Additionally, *OsAP25* and *OsAP37* display reduced expression in *udt1*, *tdr* and *ptc1*, mutants with delayed tapetal PCD (Supplementary Fig. S6b), further supporting the role of these two aspartic proteases in tapetal PCD. How UDT1 and PTC1 affect the expression of *OsAP25* and *OsAP37* remains to be elucidated.

In this study, we show that EAT1 has a unique regulatory role in tapetal PCD in comparison with previously identified proteins involved in tapetal degeneration. Unlike the expanded tapetal cells in *gamyb*, *udt1* and *tdr*[9–11], or necrosis in *ptc1* tapetum[12], *eat1-1* displays a delay in tapetal PCD without cell enlargement or necrosis-like phenotypes (Fig. 1a–l and Fig 2 and Supplementary Figs S2 and 3b). We speculate that GAMYB, UDT1 and TDR have additional roles in modulating tapetal cell size besides their roles in tapetal PCD, while the major role of EAT1 is to positively regulate tapetal PCD.

Although EAT1 interacts with TDR, TDR is unable to bind to the promoters of *OsAP25* and *OsAP37*, and EAT1 cannot bind to the promoter of *OsCP1*, a direct target of TDR[11] (data not shown). These results suggest that EAT1 and TDR may have diversified roles in the regulatory network in anther development. Furthermore, the expression of *EAT1* is obviously reduced in *tdr* (Supplementary Fig. S4h), and *eat1 tdr* double mutants exhibit the expanded tapetal cells similar to *tdr* (Fig. 1i–p), suggesting that *EAT1* acts downstream of *TDR* in regulating tapetal PCD. Consistent with this, the expression of *OsAP25* and *OsAP37* is greatly reduced in *tdr* (Supplementary Fig. S6b). It seems that EAT1 is directly regulating PCD via aspartic proteases and TDR's role in PCD is, at least in part, through EAT1 (Fig. 7).

EAT1 homologues are present in land plants and are possibly involved in male reproductive development because of their expression patterns (Supplementary Table S1). We propose that EAT1 and its close homologues have played a crucial role in land plant colonization, possibly through their involvement in the formation of the male gamete. To date, functions of *EAT1* homologues have not been reported. Our work therefore provides a clue to the possible roles of these transcriptional factors in plant programmed male development across diverse plant species.

In summary, this work has uncovered a previously unknown molecular pathway that controls programmed male reproductive development in plants, as depicted in a working model (Fig. 7). Given the importance of rice as a major crop, this finding may provide molecular basis for rational manipulation of pollen fertility to improve crop yield.

Methods

Mutant identification and molecular and phenotypic analyses. Mutant identification, plant growth, map-based cloning, phenotypic characterizations and gene expression analyses were performed using methods from our previous reports[7,11,12]. Anther staging is defined by Zhang and Wilson[45]. To fuse the *EAT1* promoter with the *GUS* (β-glucuronidase) reporter gene, a 2,102-bp fragment upstream from the start codon of *EAT1* was amplified from wild-type rice genomic DNA and cloned into the binary vector *pCAMBIA1301*. For *in situ* analysis of *EAT1*, *OsAP25* and *OsAp37*, a 491-bp *EAT1* fragment was amplified from the *EAT1* cDNA clone (AK119509, provided by RGRC); a 346-bp *OsAP25*- and a 362-bp *OsAP37*-specific fragment were amplified from wild-type rice genomic DNA. The resultant DNA fragments were cloned into *pBlueScript II SK* (*pBSK*) for producing the RNA hybridization probes.

Yeast two-hybrid assay. The MATCHMAKER GAL4 Two-Hybrid System (Clontech) was used. Because both full-length EAT1 and TDR proteins were observed to self-activate, we made a truncated EAT1, which contains the C-terminal bHLH domain (EAT1$^{\Delta}$, amino acids 255–464), and a truncated TDR containing the N-terminal bHLH domain (TDR$^{\Delta}$, amino acids 1–344). The full-length EAT1 and TDR were cloned into *pGAD-T7* (Clontech), and EAT1$^{\Delta}$ and TDR$^{\Delta}$ were cloned into *pGBK-T7* (CLONTECH), respectively. His and Ade selection and X-α-Gal filter assay were performed according to the manufacturer's instructions.

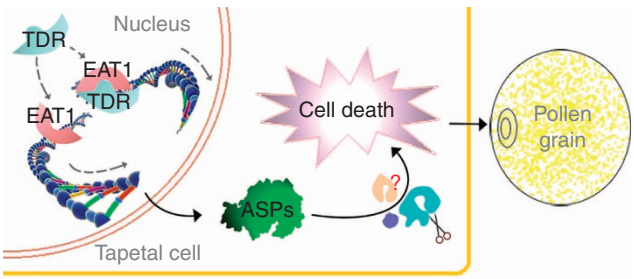

Figure 7 | A proposed model for the role of EAT1 in tapetal PCD. EAT1 acts downstream of TDR in the nucleus. EAT1 directly promotes the expression of *OsAP25* and *OsAP37* (*ASPs*), which encode aspartic proteases triggering the tapetal PCD to affect tapetal development and pollen formation.

Co-immunoprecipitation. Recombinant EAT1 expressed in *pMAL-c2X* and TDR expressed in *pET32a* (HIS-tag, Novagen) were purified using the amylose and Ni^{2+} resin, respectively. The eluent was analysed using 10% SDS–polyacrylamide gel electrophoresis, and tested using the monoclonal antibodies against maltose-binding protein (NEB, E8032) and HIS (Beyotime, AH367).

Bimolecular fluorescence complementation. The N-terminal 155 amino acids of nYFP was translationally fused to the C-terminus of full-length EAT1. The C-terminal 84 amino acids of YFP (cYFP) was translationally fused to the C-terminus of full-length TDR. The procedure of BiFC was described in Schütze *et al.*[46]

Phylogenetic analysis. Multiple alignments were performed using Muscal 3.6 (http://www.ebi.ac.uk/Tools/msa/muscle/). A phylogenetic tree was constructed with the aligned sequences from the region from the HLH to the DUF domain (correlating to amino acids 251–464 on EAT1). MEGA (version 3.0)[47] and the Neighbor-Jointing (NJ) methods were used with p-distance model and pairwise deletion and bootstrap (1000 replicates; random seed). The Max Parsimony method of MEGA was also used to support the NJ tree, using the default parameter.

qChIP-PCR. To generate EAT1 antibodies, a DNA fragment encoding an EAT1-specific peptide (amino acids 1–109) was cloned into the bacterial expression vector *pGEX-6P-1* (GE Healthcare, Cardiff, UK). The EAT1-specific peptide fused with glutathione *S*-transferase (GST) was expressed according to the manufacturer's instructions, and used to generate an EAT1-specific polyclonal antibody, using methods described in Huang *et al.*[48] The specificity of the EAT1 antibody was examined using the method described by Zhang *et al.*[49] To express the EAT1 protein, a fragment containing the C-terminal 266 aa of EAT1 was synthesized using optimized codons for *E. coli* genes (http://www.kazusa.or.jp/codon/cgi-bin/spsearch.cgi?species=Escherichia+coli&c=s) (sequence in Supplementary Table S3).

EMSA analysis. Full-length coding region of *EAT1* fused with the maltose-binding protein tag was expressed in *E. coli*, using *pMAL-c2X* (NEB, USA). DNA fragments of the *OsAP25* and *OsAP37* promoters containing putative E-boxes were amplified by OsAP25-ChIP-F and OsAP25-ChIP-R, OsAP37-ChIP-F and OsAP37-ChIP-R, respectively, and cloned into *pMD18-T* (Takara, Dalian, China). Experimental procedures of qChIP-PCR and EMSA are as described in Xu *et al.*[7]

Yeast cell-death measurement. *OsAP25* and *OsAP37* full-length coding regions containing optimized codons for expression in bacteria, yeast and plants (sequences in Supplementary Table S3, fused with c-MYC tag) were cloned into *pESC-HIS* (Agilent), using *Eco*RI and *Spe*I, and transformed into a YCA1-deficient stain, *Δyca1*. Yeast caspase assays were carried out using the system developed by Madeo *et al.*[24]. Wild-type yeast cells (BY4741) were used as the control. For yeast cell-death assay, dead cells were stained by PI and examined using flow cytometry.

Trypan blue staining of tobacco and Arabidopsis leaves. Tobacco leaves were transfected by *CAMV* 35S-driven *GFP*, *OsAP25-GFP*, or *OsAP37-GFP* for transient expression of the proteins. 10 μM PepA-P (EMD Millipore, Billerica, USA) was injected into tobacco leaves with *OsAP25-GFP* or *OsAP37-GFP*. Forty-eight hours later tobacco leaves were collected, photographed and stained with Trypan blue. c-Myc-tagged *OsAP25* and *OsAP37* (with optimized codons for expression; sequences shown in Supplementary Table S3) were cloned into *pER12*[50] using *Age*I and *Xho*I. The resulting constructs, *OsAP25-pER* and *OsAP37-pER*, are under the control of an inducible oestrogen receptor-based transactivator, XVW[50]. Fifteen-day-old *Arabidopsis Col-0* and transgenic *OsAP25-pER* and *OsAP37-pER* seedlings were treated with estradiol and stained with Trypan blue 48 h after the treatment, as described by Coll *et al.*[28] Cell death on 80 leaves and 78 cotyledons were examined for each genotype.

Plant transformation. Transient expression in tobacco leaves was performed using the method by He *et al.*[51] Agrobacterium-mediated transformation of rice and *Arabidopsis* was performed as described by Hiei *et al.*[52] and Clough and Bent[53], respectively. At least 10 independent transgenic lines for each construct were analysed.

All primer sequences are listed in Supplementary Table S4.

References

1. Scott, R., Hodge, R. & Paul, W. The molecular biology of anther differentiation. *Plant Sci.* **80,** 167–191 (1991).
2. McCormick, S. Male gametophyte development. *Plant Cell* **5,** 1265–1275 (1993).
3. Parish, R. W. & Li, S. F. Death of a tapetum: a programme of developmental altruism. *Plant Sci.* **178,** 73–89 (2010).

4. Millar, A. A. & Gubler, F. The Arabidopsis *GAMYB-like* genes, *MYB33* and *MYB65*, are microRNA-regulated genes that redundantly facilitate anther development. *Plant Cell* **17,** 705–721 (2005).
5. Zhang, W. *et al.* Regulation of Arabidopsis tapetum development and function by *DYSFUNCTIONAL TAPETUM1* (*DYT1*) encoding a putative bHLH transcription factor. *Development* **133,** 3085–3095 (2006).
6. Zhu, J. *et al.* DEFECTIVE IN TAPETAL DEVELOPMENT AND FUNCTION 1 is essential for anther development and tapetal function for microspore maturation in Arabidopsis. *Plant J.* **55,** 266–277 (2008).
7. Xu, J. *et al.* The ABORTED MICROSPORES regulatory network is required for postmeiotic male reproductive development in Arabidopsis thaliana. *Plant Cell* **22,** 91–107 (2010).
8. Wilson, Z. A., Morroll, S. M., Dawson, J., Swarup, R. & Tighe, P. J. The *Arabidopsis MALE STERILITY1* (*MS1*) gene is a transcriptional regulator of male gametogenesis, with homology to the PHD-finger family of transcription factors. *Plant J.* **28,** 27–39 (2001).
9. Aya, K. *et al.* Gibberellin modulates anther development in rice via the transcriptional regulation of GAMYB. *Plant cell 21* 1453–1472 (2009).
10. Jung, K. H. *et al.* Rice *Undeveloped Tapetum1* is a major regulator of early tapetum development. *Plant Cell* **10,** 2705–2222 (2005).
11. Li, N. *et al.* The rice *Tapetum Degeneration Retardation* gene is required for tapetum degradation and anther development. *Plant Cell* **18,** 2999–3014 (2006).
12. Li, H. *et al. PERSISTENT TAPETAL CELL1* encodes a PHD-finger protein that is required for tapetal cell death and pollen development in rice. *Plant Physiol.* **156,** 615–630 (2011).
13. Li, X. W. *et al.* Rice APOPTOSIS INHIBITOR5 coupled with two DEAD-box adenosine 5'-triphosphate-dependent RNA helicases regulates tapetum degeneration. *Plant Cell* **23,** 1416–1434 (2011).
14. Vaux, D. L. & Korsmeyer, S. J. Cell death in development. *Cell* **96,** 245–254 (1999).
15. Lam, E. Controlled cell death, plant survival and development. *Nat Rev. Mol. Cell Bio.* **5,** 305–315 (2004).
16. Lam, E. Programmed cell death in plants: orchestrating an intrinsic suicide program within walls. *Crit. Rev. Plant Sci* **27,** 413–423 (2008).
17. van Doorn, W. G. Classes of programmed cell death in plants, compared to those in animals. *J. Exp. Bot.* **62,** 4749–4761 (2011).
18. Rojo, E. *et al.* VPEγ exhibits a caspase-like activity that contributes to defense against pathogens. *Curr. Biol.* **14,** 1897–1906 (2004).
19. Chichkova, N. V. *et al.* A plant caspase-like protease activated during the hypersensitive response. *Plant Cell* **16,** 157–171 (2004).
20. Coffeen, W. C. & Wolpert, T. J. Purification and characterization of serine proteases that exhibit caspase-like activity and are associated with programmed cell death in *Avena sativa*. *Plant Cell* **16,** 857–873 (2004).
21. Hara-Nishimura, I., Hatsugai, N., Nakaune, S., Kuroyanagi, M. & Nishimura, M. Vacuolar processing enzyme: an executor of plant cell death. *Curr. Opin. Plant Biol.* **8,** 404–408 (2005).
22. Degterev, A., Boyce, M. & Yuan, J. A decade of caspases. *Oncogene* **22,** 8543–8567 (2003).
23. Woltering, E. J. Death proteases: alive and kicking. *Trends. Plant Sci.* **15,** 185–188 (2010).
24. Madeo, F. *et al.* A caspase-related protease regulates apoptosis in yeast. *Mol. Cell* **9,** 911–917 (2002).
25. Watanabe, N. & Lam, E. Two *Arabidopsis* metacaspases AtMCP1b and AtMCP2b are arginine/lysine-specific cysteine proteases and activate apoptosis-like cell death in yeast. *J. Biol. Chem.* **280,** 14691–14699 (2005).
26. Vercammen, D., Declercq, W., Vandenabeele, P. & Van Breusegem, F. Are metacaspases caspases? *J Cell Biol.* **179,** 375–380 (2007).
27. Sundström, J. F. *et al.* Tudor staphylococcal nuclease is an evolutionarily conserved component of the programmed cell death degradome. *Nat. Cell Bio.* **11,** 1347–1354 (2009).
28. Coll, N. S. *et al. Arabidopsis* type I metacaspases control cell death. *Science* **330,** 1393–1397 (2010).
29. Wong, A. H., Yan, C. & Shi, Y. Crystal structure of the yeast metacaspase Yca1. *J. Biol. Chem.* **287,** 29251–29259 (2012).
30. Hatsugai, N., Iwasaki, S., Tamura, K., Kondo, M. & Fuji, K. A novel membrane fusion-mediated plantimmunity against bacterial pathogens. *Genes Dev.* **23,** 2496–2506 (2009).
31. Phan, H. A., Iacuone, S., Li, S. F. & Parish, R. W. The MYB80 transcription factor is required for pollen development and the regulation of tapetal programmed cell death in *Arabidopsis thaliana*. *Plant Cell* **23,** 2209–2224 (2011).
32. Ge, X. *et al.* An *Arabidopsis* aspartic protease functions as an anti-cell-death component in reproduction and embryogenesis. *EMBO Rep.* **6,** 282–288 (2005).
33. Simões, I., Faro, R., Bur, D. & Faro, C. Characterization of recombinant CDR1, an *Arabidopsis* aspartic proteinase involved in disease resistance. *J. Biol. Chem.* **282,** 31358–31365 (2007).
34. Chen, J. *et al.* A triallelic system of *S5* is a major regulator of the reproductive barrier and compatibility of indica-japonica hybrids in rice. *Proc. Natl Acad. Sci USA* **105,** 11436–11441 (2008).
35. Chen, L. *et al.* Isolation and genetic analysis for rice mutants treated with ^{60}Co γ-ray. *J. Xiamen Univ. Nat. Sci.* **45,** 81–85 (2006).
36. Huysmans, S., EL-Ghazaly, G. & Smets, E. Orbicules in angiosperms: Morphology, function, distribution, and relation with tapetum types. *Bot. Rev.* **64,** 240–272 (1998).
37. Furness, C. A. & Rudall, P. J. The tapetum and systematics in monocotyledons. *Bot. Rev.* **64,** 201–239 (1998).
38. Zhang, D. B., Luo, X. & Zhu, L. Cytological analysis and genetic control of rice anther development. *J. Genet. Genomics* **38,** 379–390 (2011).
39. Nonomura, K. *et al.* The MSP1 gene is necessary to restrict the number of cells entering into male and female sporogenesis and to initiate anther wall formation in rice. *Plant Cell* **15,** 1728–1739 (2003).
40. Lee, S., Jung, K. H., An, G. & Chung, Y. Y. Isolation and characterization of a rice cysteine protease gene, *OsCP1*, using T-DNA gene-trap system. *Plant Mol. Biol.* **54,** 755–765 (2004).
41. Li, X. X. *et al.* Genome-wide analysis of basic/helix-loop-helix transcription factor family in rice and Arabidopsis. *Plant Physiol.* **141,** 1167–1184 (2006).
42. Woltering, E. J. Death proteases come alive. *Trends. Plant Sci.* **9,** 469–472 (2004).
43. Faro, C. & Gal, S. Aspartic proteinase content of the Arabidopsis genome. *Curr. Protein Pept. Sci.* **6,** 493–500 (2005).
44. Chen, J. J., Ouyang, Y. D., Wang, L., Xie, W. B. & Zhang, Q. F. Aspartic proteases gene family in rice: gene structure and expression, predicted protein features and phylogenetic relation. *Gene* **442,** 108–118 (2009).
45. Zhang, D. B. & Wilson, Z. A. Stamen specification and anther development in rice. *Chin. Sci. Bull.* **54,** 2342–2353 (2009).
46. Schütze, K., Harter, K. & Chaban, C. Bimolecular fluorescence complementation (BiFC) to study protein–protein interactions in living plant cells. *Methods Mol. Biol.* **479,** 189–202 (2009).
47. Tamura, K., Dudley, J., Nei, M. & Kumar, S. MEGA4: Molecular Evolutionary Genetics Analysis (MEGA) Software Version 4.0. *Mol. Biol. Evol.* **24,** 1596–1599 (2007).
48. Huang, Y. H. *et al.* Production of FaeG, the major subunit of K88 fimbriae, in transgenic tobacco plants and its immunogenicity in mice. *Infect. Immun.* **71,** 5436–5439 (2003).
49. Zhang, H. *et al. Carbon Starved Anther* encodes a MYB domain protein that regulates sugar partitioning required for rice pollen development. *Plant Cell* **22,** 672–689 (2010).
50. Zuo, J. R., Niu, Q. W. & Chua, N. H. Technical advance: an estrogen receptor-based transactivator XVE mediates highly inducible gene expression in transgenic plants. *Plant J.* **24,** 265–273 (2000).
51. He, X. F., Fang, Y. Y., Feng, L. & Guo, H. S. Characterization of conserved and novel microRNAs and their targets, including a TuMV-induced TIR-NBS-LRR class R gene-derived novel miRNA in Brassica. *FEBS Lett.* **582,** 2445–2452 (2008).
52. Hiei, Y., Komari, T. & Kubo, T. Transformation of rice mediated by *Agrobacterium tumefaciens*. *Plant Mol. Biol.* **35,** 205–218 (1997).
53. Clough, S. J. & Bent, A. F. Floral dip: a simplied method for Agrobacterium-mediated transformation of *Arabidopsis thaliana*. *Plant J.* **16,** 735–743 (1998).

Acknowledgements

Dabing Zhang would like to dedicate this article to his PhD advisor, Professor Mengmin Hong, who passed away on November 13, 2012. We gratefully acknowledge Nuria Sanchez Coll for critical reading of this manuscript; Dasheng Zhang, Jie Xu and Zheng Yuan for helpful discussions; Zhijing Luo and Mingjiao Chen for growing rice plants; Changsong Yin for *in situ* analysis; Instrument Sharing and Technical Service Platform, School of Life Sciences and Biotechnology and Biotechnology and Instrumental Analysis Center of SJTU for SEM and TEM observation; and Qian Luo for flow cytometry. We thank Bin Han for providing the bacterial artificial chromosome clone; the RGRC for providing the cDNA clone and the *eat1-2* and *eat1-3* mutants; Frank Madeo for providing yeast strains (BY4741 and *Δyca1*) and the *pESC-HIS* vector; Richard Jefferson for the vector *pCAMBIA1301*; and Hongquan Yang for the *pHB* vector. This work was supported by funds from the National Key Basic Research Developments Program, Ministry of Science and Technology, China (2013CB126902; 2009CB941500); 863 Hitech Project, Ministry of Science and Technology, China (2012AA10A302; 2011AA10A101); National Natural Science Foundation of China (31110103915; 31171518; 30830014); the Science and Technology Commission of Shanghai Municipality (10JC1406400; 10DZ2294100; 11JC1404900); and National Transgenic Major Program (2011ZX08009-003-003) to D.Z.

Author contributions

N.N. carried out major parts of all experiments. X.Y. performed the primary mapping of *eat1-1*. W.J. did caspase activity analysis. J.H. and Z.A.W. helped in designing the work

on caspase activity assays and preparation of the manuscript. D.Z. and W.L. designed the study and prepared the manuscript.

Additional information

Supplementary Information accompanies this paper at http://www.nature.com/naturecommunications

Competing financial interests: The authors declare no competing financial interests.

Data deposition statement (accession numbers): *OsAP25*, LOC_Os03g08790 (http://www.gramene.org/) or Os03g0186900 (http://rapdb.dna.affrc.go.jp/); *OsAP37*, LOC_Os04g37570 or Os04g0448500; *OsAP19*, LOC_Os02g27360 or Os02g0473200; *MSP1*, LOC_Os01g68870 or Os01g0917500; *GAMYB*, LOC_Os01g59660 or Os01g0812000; *UDT1*, LOC_Os07g36460 or Os07g0549600; *TDR*, LOC_Os02g02820 or Os02g0120500; *PTC1*, LOC_Os09g27620 or Os09g0449000; *API5*, LOC_Os02g20930 or Os02g0313400; *OsCP1*, LOC_Os04g57490 or Os04g0670500. All of peptides included in the NJ tree were from NCBI.

How to cite this article: Niu, N. *et al.* EAT1 promotes tapetal cell death by regulating aspartic proteases during male reproductive development in rice. *Nat. Commun.* 4:1445 doi: 10.1038/ncomms2396 (2013).